JOURNAL OF Materials CHEMISTRY

Formation and structure of aluminium alkyl phosphates

Hidekazu Tanaka*† and Masatoshi Chikazawa

Department of Industrial Chemistry, Faculty of Engineering, Tokyo Metropolitan University, 1-1 Minami-ohsawa, Hachioji-shi, Tokyo, 192-0397, Japan

Received 19th March 1999, Accepted 18th August 1999

Aluminium alkyl phosphates (AlAPs) synthesized by the reaction of $Al(NO_3)_3 \cdot 9H_2O$ with monohexyl, monooctyl or monodecyl phosphates in aqueous media have been characterized by various means. The XRD patterns of the AlAPs showed one strong and two weak diffraction peaks at $2\theta < 15^\circ$. The plate-like AlAP particles prepared using octyl phosphate gave rise to lattice patterns having uniform alternating spacings of *ca.* 1.1 and 1.5 nm. When treated at 1000 °C, AlAP samples were converted into tridymite $AlPO_4$. The Al/P molar ratios of AlAP samples approximated to unity and their chemical formula can be written as $(ROPO_3)Al(OH) \cdot 1.2H_2O$. These facts suggest that the AlAPs are composed of alternating bimolecular layers of alkyl phosphates and a hydrated aluminium phosphate phase.

Introduction

Alumina (Al_2O_3)[1] and calcium hydroxyapatite ($Ca_{10}(PO_4)_6(OH)_2$: CaHAP)[2] are used as artificial teeth and bones owing to their excellent biocompatibility and the fact that they are completely dissolved during the restoration of hard tissues. Therefore, information on the interaction between metal ions eluted from these materials and biomolecules is of great interest to medical and dental therapists. Alkyl phosphates are major organic phosphates in animals, *e.g.*, in vesicle membranes, DNA and ATP, and are sources of hard tissues. Previously, we studied the interactions between Ca^{2+} ions and alkyl phosphate ions[3] as well as between CaHAP and alkyl phosphates,[4–6] and indicated that a layered structure composed of alternating bimolecular layers of alkyl phosphates and a dicalcium phosphate dihydrate (DCPD)-like phase is formed. However, to our knowledge, no study has been reported on the interaction between Al^{3+} and alkyl phosphate ions except for the studies by Fukasawa and Tsutsumi,[7,8] Sanchez-Camazano and Sanchez-Martin[9] and our previous paper.[10] Fukasawa and Tsutsumi prepared a binary system of aluminium salts of dihexadecyl phosphate (C_{16}DP-Al) and *n*-hexadecane and suggested the chemical composition of C_{16}DP-Al to be $[(C_{16}H_{33}O)_2OPO]_3Al$.[7,8] Sanchez-Camazano and Sanchez-Martin treated kaolinite with trimethyl phosphate in hot water and found that the silicate structure of kaolinite is completely destroyed and that aluminium alkyl phosphate $[Al(CH_3)_6(PO_4)_3]$ is formed.[9] Nevertheless, the structure and mechanism of formation of these materials have not been fully explored. Previously, we modified amorphous aluminium phosphate ($AlPO_4$) with monohexyl, monooctyl and monodecyl phosphates and found that a layered structure composed of bimolecular layers of alkyl phosphates and aluminium phosphate phases was formed on the $AlPO_4$ surface.[10] The formation mechanism of the layered structure was interpreted in terms of the surface of $AlPO_4$ being dissolved by acidic alkyl phosphate solutions to yield Al^{3+} and alkyl phosphate ions, which react together, leading to deposition of aluminium alkyl phosphates on the $AlPO_4$ surface. Furthermore, many researchers have studied the influence of Al^{3+} ions on diseases such as Alzheimer's syndrome.[11–18] Nevertheless, the detailed structure and formation mechanism of the layered structure referred to above, as well as the relation between Al^{3+} ions and Alzheimer's syndrome have not been satisfactorily established.

This study aimed to clarify the interaction between Al^{3+} and alkyl phosphate ions. We synthesized aluminium alkyl phosphates (AlAPs) by reaction of Al^{3+} ions with monohexyl, monooctyl and monodecyl phosphate ions and the resulting materials were characterized by XRD, TG–DTA, FTIR, ICP and CHN elemental analysis. Based on the results obtained, the formation mechanism and structure of the AlAPs are discussed. Moreover, the results obtained may not only elucidate the modification mechanism of $AlPO_4$ with alkyl phosphates but may also clarify the relation between Al^{3+} ions and Alzheimer's syndrome.

Experimental

Materials

The aluminium alkyl phosphates were prepared by a wet method under the same conditions as used for the preparation of calcium alkyl phosphates.[3] $Al(NO_3)_3 \cdot 9H_2O$ (6.1×10^{-3} mol) was dissolved in 400 ml of distilled and deionized CO_2-free water in a polypropylene vessel by stirring for 1 h. After stirring, 100 ml solutions containing 6.1×10^{-3} mol of monohexyl, monooctyl or monodecyl phosphates were added. The resulting suspensions were stirred for 1 h and then aged at 100 °C for 24 h in an air oven and the precipitates filtered off, washed with distilled water and acetone, and finally dried in a vacuum desiccator for 1 day at room temperature. The materials obtained using monohexyl, monooctyl and monodecyl phosphates are denoted AlAP-6, AlAP-8 and AlAP-10, respectively.

Monohexyl, monooctyl and monodecyl phosphates were synthesized by reacting pyrophosphoric acid with 1-hexanol, 1-octanol and 1-decanol, respectively.[19] The purity of the alkyl phosphates was established by CHN elemental analysis and FTIR spectroscopy. All the chemicals were reagent grade and used without further purification.

Characterization

The prepared samples were characterized by a variety of techniques. Powder X-ray diffraction (XRD) patterns were obtained on a Rigaku diffractometer with Ni-filtered Cu-Kα radiation (30 kV, 15 mA). Particle morphology was observed using a JEOL transmission electron microscope (TEM).

†Present address: School of Chemistry, Osaka University of Education, 4-698-1 Asahigaoka, Kashiwara-shi, Osaka 582-8582, Japan. Fax: +81-729-78-3394; E-mail: hidesan@cc.osaka-kyoiku.ac.jp

Thermal gravimetry (TG) and differential thermal analysis (DTA) curves were recorded on a Seiko thermoanalyzer at a heating rate of 5 °C min^{-1} under both air and N_2 streams. Carbon contents were assayed by a Perkin-Elmer CHN elemental analyzer whereas Al and P contents were determined with a Perkin-Elmer inductively coupled plasma (ICP) spectrometer after dissolving the samples in HNO_3. Transmission IR spectra (KBr disks) were measured on a JASCO Fourier transform infrared (FTIR) spectrometer. Transmission IR spectra *in vacuo* using a self-supporting disk method were recorded on a Nicolet Fourier transform infrared (FTIR) spectrometer with a triglycine sulfate (TGS) sensor.

Results and discussion

XRD and TEM

Fig. 1 shows the XRD patterns of AlAP-6, -8 and -10 while diffraction angles 2θ and *d*-spacings are listed in Table 1. All the patterns show one strong diffraction peak and two weak ones at $2\theta < 15°$. The positions of these peaks shift to lower diffraction angles and their intensities are weakened upon increasing the carbon number of the phosphates, in a similar manner as found for modified $AlPO_4$ with alkyl phosphates, as reported previously.[10] These facts suggest that the AlAPs are composed of a layered structure as well as the surface phase of the modified $AlPO_4$ particles.[10] No peaks were observed for any sample for $2\theta > 15°$.

The AlAP particles were thin plates and of similar morphology for the three different AlAP samples. Furthermore, the layered structure suggested by XRD is evident in Fig. 2 which shows a part of a micrograph of AlAP-8; lattice patterns having uniform alternating spacings of *ca.* 1.1 nm (white zone) and *ca.* 1.5 nm (black zone) can be clearly seen. Consequently, the layered structure of the AlAPs enables understanding of the formation mechanism of the layered structure on the modified $AlPO_4$ surface.

Thermal analysis

Fig. 3 shows TG and DTA curves of AlAP-6, -8 and -10 obtained in a flow of air. All the TG curves show two weight losses at *ca.* 100 °C (step 1) and *ca.* 300 °C (step 2) accompanied by an endothermic peak and three exothermic peaks, respectively. On increasing the carbon number of the alkyl phosphate, the weight loss value of step 1 decreases while that at step 2 increases. Alkyl groups in AlAP-6, -8 and -10 estimated from CHN elemental analysis correspond to 37.1, 39.0 and 41.1 wt%, respectively, close to the weight loss values of 36.9, 38.4 and 40.6 wt% in the TG curves for step 2. To elucidate the origin of each of the steps, TG and DTA curves were also recorded under N_2. All the TG curves in N_2 were almost the same as those measured in air, while the exothermic peaks corresponding to step 2 became endothermic as expected for desorption of alkyl groups. It has been reported that the thermal decomposition of surface alkyl groups on silica gel in the absence of O_2 occurs by a mechanism whereby SiO–C bonds are broken and Si–OH bonds are generated yielding alkenes.[20] Analogously thermal decomposition of alkyl groups

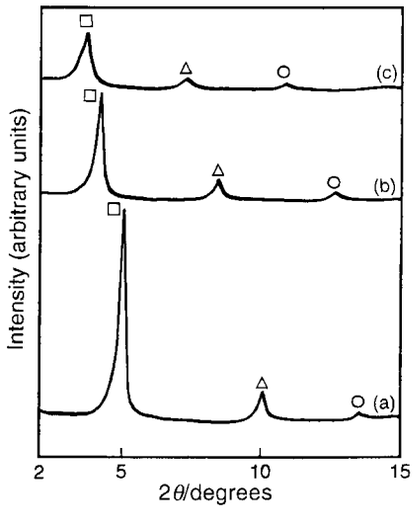

Fig. 1 XRD patterns of AlAPs: (a) AlAP-6, (b) AlAP-8, (c) AlAP-10.

Table 1 Diffraction peak positions (Fig. 1) of AlAP samples

Sample	2θ/degrees	*d*-spacing/nm
AlAP-6	5.0	1.8
	10.0	0.8
	15.1	0.6
AlAP-8	4.2	2.1
	8.4	1.1
	12.7	0.7
AlAP-10	3.7	2.4
	7.3	1.2
	10.9	0.8

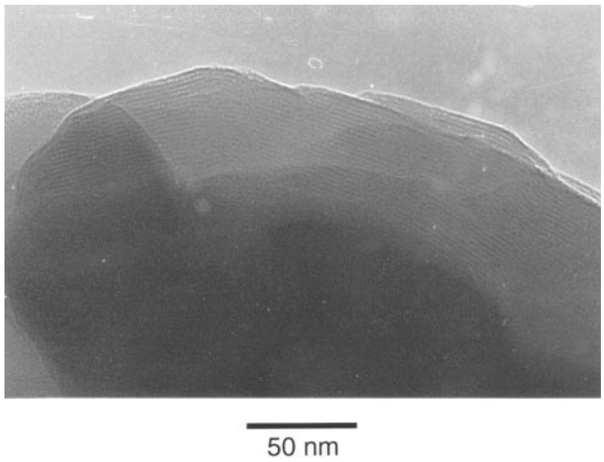

Fig. 2 TEM image of AlAP-8.

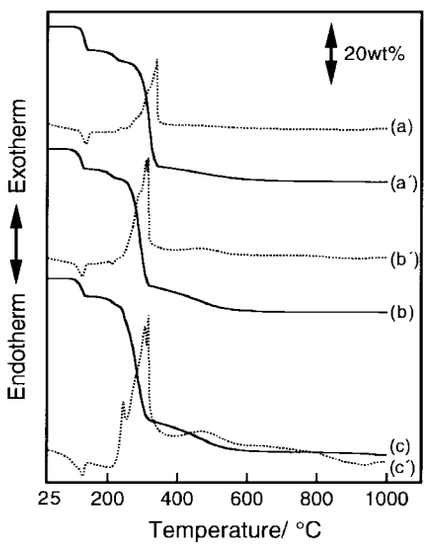

Fig. 3 TG–DTA curves in air of AlAPs: [(a), (a′)] AlAP-6, [(b), (b′)] AlAP-8, [(c), (c′)] AlAP-10. The solid and dotted lines refer to TG and DTA curves, respectively.

of AlAPs in an N_2 stream would proceed *via* the reaction below (shown for AlAP-6)

$$P{-}O{-}C_6H_{13} \rightarrow P{-}OH + CH_2{=}CH{-}C_4H_9$$

Accordingly, steps 1 and 2 observed in air can be ascribed to the removal of adsorbed and/or bound H_2O and to combustion of alkyl groups of the phosphates, respectively. The existence of H_2O in the samples was confirmed by FTIR as described below.

To corroborate the thermal transformation of the AlAPs, XRD patterns of AlAP-6 treated in air at elevated temperatures for 2 h were recorded and are shown in Fig. 4. Upon treatment at 400 °C, the three strong diffraction peaks observed in Fig. 1 completely disappear and the material becomes amorphous [Fig. 4(b)]. Upon further heating to 1000 °C, sharp peaks appear at $2\theta = 20.5$, 21.6, 23.1 and 35.7° [Fig. 4(c)], which can be assigned to tridymite $AlPO_4$ (JCPDS 15-254).

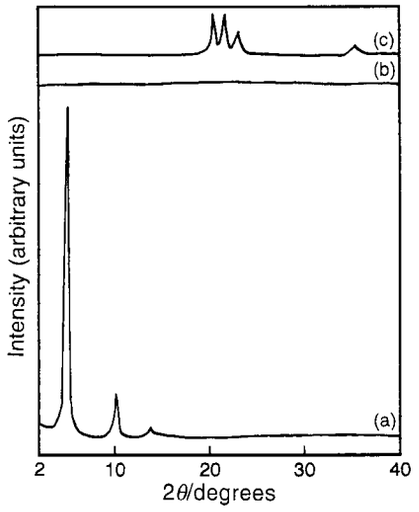

Fig. 4 XRD patterns of AlAP-6 treated in air at various temperatures: (a) untreated, (b) 400 °C, (c) 1000 °C.

IR spectroscopy

Fig. 5 shows IR spectra (KBr disk) of AlAP-10 along with AlAP-10 heated at 400 °C in air for 2 h. The spectrum of the untreated sample [Fig. 5(a)] shows absorption bands at 3659, 3633, 3453, 2957, 2930 and 2860 cm^{-1}. To assign the first two bands, the IR spectrum *in vacuo* of AlAP-10 outgassed at 100 °C for 2 h was measured using a self-supporting disk method and H–D exchange of this material was carried out by repeating D_2O adsorption–desorption cycles. After this D_2O treatment, the bands at 3659 and 3633 cm^{-1} were weakened, while new two bands appeared at 2700 and 2681 cm^{-1} (spectrum not shown). The wavenumber ratios of these bands were 1.355 (3659/2700) and 1.355 (3633/2681), close to the theoretical ratio (νOH/νOD) of 1.374. Moreover, the 3659 and 3633 cm^{-1} bands are close to the 3650 cm^{-1} band due to Al–OH detected for aluminium methylphosphonate [Al(OH)-$PO_3Me{\cdot}H_2O$] prepared by the reaction of $Al(OH)_3{\cdot}H_2O$ with methylphosphonate.[21] Hence, the bands at 3659 and 3633 cm^{-1} can be ascribed to the Al–OH stretching vibration modes of AlAP-10. The 3453 cm^{-1} band is assigned to the vibration mode of OH groups of bound or adsorbed water within AlAP-10 and the 2957, 2930 and 2860 cm^{-1} bands can be assigned to the stretching vibration modes of CH groups. Besides these bands, there are further absorptions at 1635, 1467, 1141, 1097, 1066, 1018 and 522 cm^{-1}. The 1635 cm^{-1} band is assigned to the deformation vibration mode of H_2O, the 1467 cm^{-1} band to the deformation vibration mode of

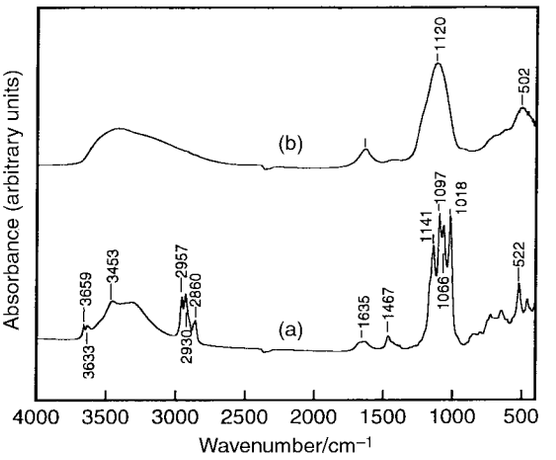

Fig. 5 IR spectra of AlAP-10: (a) untreated and (b) treated at 400 °C in air.

$-(CH_2)_9-$ and the 1141, 1097, 1066, 1018 and 522 cm^{-1} bands to the P–O stretching vibration modes of P–O–C groups. Upon treatment at 400 °C, the bands due to Al–OH groups, CH groups and P–O–C groups virtually disappear whilst bands of the P–O stretching vibration mode of PO_4^{3-} ions emerge at 1120 and 502 cm^{-1} [Fig. 5(b)].

Formation mechanism and thermal decomposition of AlAPs in air

From the above results, we can propose a mechanism of formation and thermal decomposition in air of AlAP as shown in Scheme 1 for AlAP-10. Reaction (1) is the reaction of Al^{3+} ions with decyl phosphate ions to yield AlAP-10: the presence of H_2O in the sample was confirmed by TG–DTA and FTIR. The Al/P molar ratios of AlAP-6, -8 and -10 assayed by ICP were 0.96, 0.95 and 0.95, respectively which approximated to unity and were clearly different from a value of 0.33 proposed by Fukasawa and Tsutsumi[7,8] and Sanchez-Camazano and Sanchez-Martin.[9] The amount of H_2O in AlAP-6, -8 and -10 estimated from the TG curves were 4.81, 4.39 and 4.02 mmol g^{-1}, respectively. Therefore, the chemical formula of AlAP-6, -8 and -10 can be written as $(C_6H_{13}OPO_3)Al(OH){\cdot}1.2H_2O$, $(C_8H_{17}OPO_3)Al(OH){\cdot}1.2H_2O$ and $(C_{10}H_{21}OPO_3)Al(OH){\cdot}1.2H_2O$, respectively. The presence of Al–OH groups in the materials was detected by FTIR. Upon treatment at 100 °C, the hydrated H_2O molecules are removed

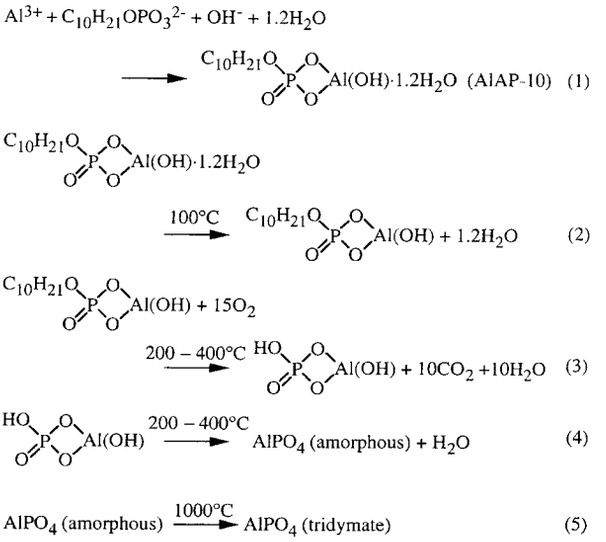

Scheme 1 Formation mechanism and thermal decomposition of AlAP-10 in air.

via reaction (2). Heating at 200–400 °C leads to combustion of the decyl groups to form $AlHPO_4(OH)$ *via* reaction (3). Amorphous $AlPO_4$ is produced by reaction of P–OH and Al–OH groups in $AlHPO_4(OH)$ *via* reaction (4). Upon treatment at 1000 °C, the amorphous $AlPO_4$ is crystallized to give tridymite $AlPO_4$ *via* reaction (5).

Layered structure

As is shown in Fig. 1 and Table 1, the XRD pattern of AlAP-10 shows three diffraction peaks at $2\theta = 3.7°$ ($d = 2.4$ nm), 7.3° (1.2 nm) and 10.9° (0.8 nm), for which the first peak is extremely strong and the *d*-spacing ratio of these peaks is 2.4 : 1.2 : 0.8, corresponding to 1 : 1/2 : 1/3. Similar results were obtained for AlAP-6 and -8 (Table 1). These results reveal that the AlAPs consist of a highly ordered layer structure. Fig. 6 plots *d*-spacings of these diffraction peaks *vs.* the length of the alkyl groups of the phosphates in terms of carbon number and clearly shows that the *d*-spacings linearly increase with the length of the alkyl groups of the phosphates. In our previous study, calcium alkyl phosphates consisting of alternating bimolecular layers of alkyl phosphates and a DCPD-like phase were prepared and it was shown that the *d*-spacings of the bimolecular layer of alkyl phosphates also linearly increased with the carbon number of the alkyl group of the phosphate.[3] Thus, the structure of the AlAPs appears to resemble that of calcium alkyl phosphates. The increment of *d*-spacing per carbon estimated from the slope of the straight line for the square symbols in Fig. 6 is 1.63 nm which is clearly different from an expected value of 2.50 nm for a bimolecular layer of alkyl groups obtained assuming the C–C bond and C–C–C angle to be 0.154 nm and 109°, respectively. Therefore, it appears that the alkyl groups of the phosphates are inclined at an angle of 40° to the layers. From this result, the thickness of the bimolecular layer of octyl groups is 1.14 nm which is close to the value of *ca.* 1.1 nm for the lattice spacing estimated from the TEM image for AlAP-8 shown in Fig. 2. Consequently, the *d*-spacings represented by open squares in Fig. 6 correspond to the thickness of the bimolecular layer of alkyl phosphates and the three diffraction peaks in Fig. 1 would arise from reflections such as (001) or (0*k*0) and higher order terms.

Based on the obtained results, we can propose a layered structure of AlAP as shown in Fig. 7 which depicts a schematic layered structure of AlAP-10. All the decyl groups of the phosphates are inclined at an angle of 40° to the surface of the hydrated aluminium phosphate phase. A bimolecular layer of decyl groups is formed between the hydrated aluminium phosphate phases owing to the hydrophobic nature of the decyl groups. The alternating bimolecular layer of alkyl phosphates and hydrated aluminium phosphate phase self-assemble into a multilayer. It has been reported that aluminium methylphosphonate consists of parallel chains of aluminium–oxygen octahedra linked *via* bridging oxygens and methylphosphonate groups to give inorganic sheets partially covered on both surfaces by methyl groups.[21] In order to obtain a more detailed structure of the hydrated aluminium phosphate phase, preparation of single-crystal AlAP samples is required. Unfortunately such preparation of single crystals has yet to be achieved.

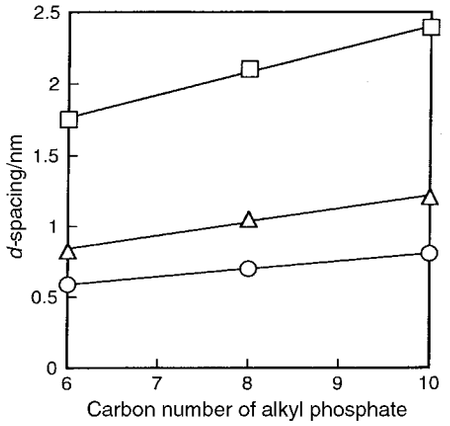

Fig. 6 Plots of *d*-spacing estimated from the XRD peaks in Fig. 1 as a function of carbon number of alkyl phosphates. For guide to symbols see Fig. 1.

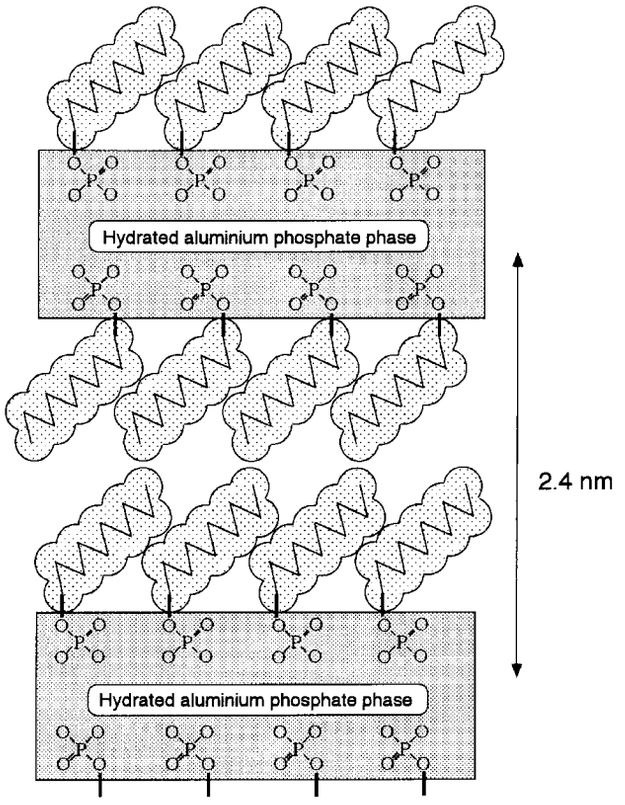

Fig. 7 Schematic structure of AlAP-10.

Conclusions

The results obtained in the present study can be summarized as follows. Multilayer aluminium hexyl, octyl and decyl phosphates, composed of alternating bimolecular layers of alkyl phosphates and the hydrated aluminium phosphate phase, were prepared by the reaction of $Al(NO_3)_3 \cdot 9H_2O$ with monohexyl, monooctyl and monodecyl phosphates in aqueous media. The structure of the AlAPs corresponds closely to that of the surface phase of $AlPO_4$ modified with alkyl phosphates in our previous study.[10] The chemical formula of the AlAPs can be written as $(ROPO_3)Al(OH) \cdot 1.2H_2O$. The alkyl groups of the phosphates were removed at 400 °C and the materials were transformed into amorphous $AlPO_4$. Upon treatment at 1000 °C, the amorphous $AlPO_4$ was crystallized to tridymite $AlPO_4$.

Acknowledgements

The authors thank Mr. Masato Wakamura of Fujitsu Laboratories for his help with ICP measurements.

References

1 H. Hede and U. Hoffmann, *Ber. Dtsch. Keram. Ges.*, 1972, **49**, 185.
2 E. A. Monroe, W. Votava, D. B. Bass and J. McMullen, *J. Dent. Res.*, 1971, **50**, 860.

3 H. Tanaka, T. Watanabe, M. Chikazawa, K. Kandori and T. Ishikawa, *Colloids Surf. A.*, 1998, **139**, 341.
4 T. Ishikawa, H. Tanaka, A. Yasukawa and K. Kandori, *J. Mater. Chem.*, 1995, **5**, 1963.
5 H. Tanaka, A. Yasukawa, K. Kandori and T. Ishikawa, *Langmuir*, 1997, **13**, 821.
6 H. Tanaka, A. Yasukawa, K. Kandori and T. Ishikawa, *Colloids Surf. A*, 1997, **125**, 53.
7 J. Fukasawa and H. Tsutsumi, *J. Colloid Interface Sci.*, 1991, **143**, 69.
8 J. Fukasawa and H. Tsutsumi, *Yukagaku*, 1987, **36**, 865.
9 M. Sanchez-Camazano and M. J. Sanchez-Martin, *Clays Clay Miner.*, 1994, **42**, 221.
10 H. Tanaka and M. Chikazawa, *Mater. Res. Bull.*, in press.
11 R. W. Shin, *Gerontology*, 1997, **43**, 16.
12 C. N. Martyn, D. N. Coggon, H. Inskip, R. F. Lacey and W. F. Young, *Epidemiology*, 1997, **8**, 281.
13 E. Bjertness, J. M. Candy, A. Torvik, P. Ince, F. McArthur, G. A. Taylor, S. W. Johansen, J. Alexander, J. K. Gronnesby, L. S. Bakketeig and J. A. Edwardson, *Alzheimer Dis. Assoc. Disord.*, 1996, **10**, 171.
14 W. F. Forbes and D. R. McLachlan, *J. Epidemiol Community Health*, 1996, **50**, 401.
15 R. A. Armstrong, S. J. Winsper and J. A. Blair, *Dementia*, 1996, **7**, 1.
16 J. Savory, C. Exley, W. F. Forbes, Y. Huang, J. G. Joshi, T. Kruck, D. R. McLachlan and I. Wakayama, *J. Toxicol. Environ. Health*, 1996, **46**, 615.
17 D. R. McLachlan, C. Bergeron, J. E. Smith, D. Boomer and S. L. Rifat, *Neurology*, 1996, **46**, 401.
18 H. Yoshida and F. Yoshimasu, *Nippon Rinsho*, 1996, **54**, 111.
19 A. K. Nelson and A. D. F. Toy, *US Pat.*, 3,146,255, 25 August 1964.
20 H. Utsugi, *Hyomen*, 1978, **16**, 525.
21 L. J. Sawers, V. J. Carter, A. R. Armstrong, P. G. Bruce, P. A. Wright and B. E. Gore, *J. Chem. Soc., Dalton Trans.*, 1996, 3159.

Paper 9/06612H